

Using Multipoles of the Correlation Function to Measure $H(z)$, $D_A(z)$, and $\beta(z)$ from Sloan Digital Sky Survey Luminous Red Galaxies

Chia-Hsun Chuang,^{*} † and Yun Wang

¹ Instituto de Física Teórica, (UAM/CSIC), Universidad Autónoma de Madrid, Cantoblanco, E-28049 Madrid, Spain

² Homer L. Dodge Department of Physics & Astronomy, Univ. of Oklahoma, 440 W Brooks St., Norman, OK 73019, U.S.A.

10 November 2018

ABSTRACT

Galaxy clustering data can be used to measure the cosmic expansion history $H(z)$, the angular-diameter distance $D_A(z)$, and the linear redshift-space distortion parameter $\beta(z)$. Here we present a method for using effective multipoles of the galaxy two-point correlation function ($\hat{\xi}_0(s)$, $\hat{\xi}_2(s)$, $\hat{\xi}_4(s)$, and $\hat{\xi}_6(s)$, with s denoting the comoving separation) to measure $H(z)$, $D_A(z)$, and $\beta(z)$, and validate it using LasDamas mock galaxy catalogs. Our definition of effective multipoles explicitly incorporates the discreteness of measurements, and treats the measured correlation function and its theoretical model on the same footing. We find that for the mock data, $\hat{\xi}_0 + \hat{\xi}_2 + \hat{\xi}_4$ captures nearly all the information, and gives significantly stronger constraints on $H(z)$, $D_A(z)$, and $\beta(z)$, compared to using only $\hat{\xi}_0 + \hat{\xi}_2$.

We apply our method to the sample of luminous red galaxies (LRGs) from the Sloan Digital Sky Survey (SDSS) Data Release 7 (DR7) without assuming a dark energy model or a flat Universe. We find that $\hat{\xi}_4(s)$ deviates on scales of $s < 60$ Mpc/ h from the measurement from mock data (in contrast to $\hat{\xi}_0(s)$, $\hat{\xi}_2(s)$, and $\hat{\xi}_6(s)$), thus we only use $\hat{\xi}_0 + \hat{\xi}_2$ for our fiducial constraints. We obtain $\{H(0.35), D_A(0.35), \Omega_m h^2, \beta(z)\} = \{79.6_{-8.7}^{+8.3} \text{ km s}^{-1} \text{ Mpc}^{-1}, 1057_{-87}^{+88} \text{ Mpc}, 0.103 \pm 0.015, 0.44 \pm 0.15\}$ using $\hat{\xi}_0 + \hat{\xi}_2$. We find that $H(0.35) r_s(z_d)/c$ and $D_A(0.35)/r_s(z_d)$ (where $r_s(z_d)$ is the sound horizon at the drag epoch) are more tightly constrained: $\{H(0.35) r_s(z_d)/c, D_A(0.35)/r_s(z_d)\} = \{0.0437_{-0.0043}^{+0.0041}, 6.48_{-0.43}^{+0.44}\}$ using $\hat{\xi}_0 + \hat{\xi}_2$.

Key words: cosmology: observations, distance scale, large-scale structure of Universe

1 INTRODUCTION

The cosmic large-scale structure from galaxy redshift surveys provides a powerful probe of dark energy and the cosmological model that is highly complementary to the cosmic microwave background (CMB) (Bennett et al. 2003), supernovae (SNe) (Riess et al. 1998; Perlmutter et al. 1999), and weak lensing (Wittman et al. 2000; Bacon, Refregier, & Ellis 2000; Kaiser, Wilson, & Luppino 2000; Van Waerbeke et al. 2000). The scope of galaxy redshift surveys has dramatically increased in the last decade. The PSCz surveyed $\sim 15,000$ galaxies using the Infrared Astronomical Satellite (IRAS) (Saunders et al. 2000), the 2dF Galaxy Redshift Survey (2dFGRS) obtained 221,414 galaxy redshifts (Colless et al. 2001, 2003), and the Sloan Digital Sky Survey (SDSS) has col-

lected 930,000 galaxy spectra in the Seventh Data Release (DR7) (Abazajian et al. 2009). WiggleZ has collected 240,000 emission-line galaxies at $0.5 < z < 1$ over 1000 square degrees (Blake et al. 2009; Parkinson et al. 2012), and BOSS is surveying 1.5 million luminous red galaxies (LRGs) at $0.1 < z < 0.7$ over 10,000 square degrees (Eisenstein et al. 2011). The BOSS data set has been made publicly available recently in SDSS data release 9 (Anderson et al. 2012; Manera et al. 2012; Nuza et al. 2012; Reid et al. 2012; Samushia et al. 2012; Tojeiro et al. 2012). The planned space mission Euclid¹ will survey over 60 million emission-line galaxies at $0.7 < z < 2$ over 15,000 square degrees (Cimatti et al. 2009; Wang et al. 2010; Laureijs et al. 2011).

Large-scale structure data from galaxy redshift surveys can be analyzed using either the power spectrum or the correlation function. Although these two methods are Fourier trans-

* E-mail: chia-hsun.chuang@uam.es

† MultiDark Fellow

¹ <http://www.euclid-emc.org/>

forms of one another, the analysis processes are quite different and the results cannot be converted using Fourier transform directly because of the finite size of the survey volume. The SDSS data have been analyzed using both the power spectrum method (see, e.g., Tegmark et al. 2004; Hutsi 2005; Padmanabhan et al. 2007; Blake et al. 2007; Percival et al. 2007, 2010; Reid et al. 2010; Montesano et al. 2011), and the correlation function method (see, e.g., Eisenstein et al. 2005; Okumura et al. 2008; Cabre & Gaztanaga 2009; Martinez et al. 2009; Sanchez et al. 2009; Kazin et al. 2010a; Chuang, Wang, & Hemantha 2012; Samushia et al. 2011; Padmanabhan et al. 2012).

The power of galaxy clustering as a dark energy probe lies in the fact that the Hubble parameter, $H(z)$, and the angular diameter distance, $D_A(z)$, can in principle be extracted simultaneously from data through the measurement of the baryon acoustic oscillation (BAO) scale in the radial and transverse directions (Blake & Glazebrook 2003; Seo & Eisenstein 2003; Wang 2006). Okumura et al. (2008) concluded that SDSS DR3 LRG data were not sufficient for measuring $H(z)$ and $D_A(z)$; they derived constraints on cosmological parameters assuming that dark energy is a cosmological constant. Cabre & Gaztanaga (2009) measured the linear redshift space distortion parameter β , galaxy bias, and σ_8 from SDSS DR6 LRGs. Gaztanaga, Cabre, & Hui (2009) obtained a measurement of $H(z)$ by measuring the peak of the correlation function along the line of sight. However, Kazin et al. (2010b) showed that the amplitude of the line-of-sight peak is consistent with sample variance.

In our previous paper (Chuang & Wang 2012), we presented a method to measure $H(z)$ and $D_A(z)$ from the full 2D correlation function of a sample of SDSS DR7 LRGs (Eisenstein et al. 2001) without assuming a dark energy model or a flat Universe. It is also the first application which includes the geometric distortion (also known as Alcock-Paczynski test, see Alcock & Paczynski (1979)) on the galaxy clustering data at large scales. We demonstrated the feasibility of extracting $H(z)$ and $D_A(z)$ by applying our method to individual LasDamas mock catalogs which mimic the galaxy sample and survey geometry of the observational data we used. In this paper, we extend our method by exploring the use of the multipoles of the correlation function to measure $H(z)$, $D_A(z)$, and $\beta(z)$. The obvious advantage of using multipoles of the correlation function instead of the full 2D correlation function is the reduced number of data points used to obtain similar amounts of information. In Section 2, we introduce the galaxy sample used in our study. In Section 3, we describe the details of our method. In Section 4, we present our results. In Section 5, we apply some systematic tests to our measurements. We summarize and conclude in Sec. 6.

2 DATA

The SDSS-I/II has observed one-quarter of the entire sky and performed a redshift survey of galaxies, quasars and stars in five passbands u, g, r, i , and z with a 2.5m telescope (Fukugita et al. 1996; Gunn et al. 1998, 2006). We use the public catalog, the NYU Value-Added Galaxy Catalog (VAGC) (Blanton et al. 2005), derived from the SDSS II final public data release, Data Release 7 (DR7) (Abazajian et al. 2009). We select our LRG sample from the NYU VAGC with the flag *primTarget* bit mask set to 32. K-corrections have been applied to the galaxies with a fiducial model (Λ CDM with $\Omega_m = 0.3$ and $h = 1$), and the selected galaxies are required to have rest-frame g -band absolute magni-

tudes $-23.2 < M_g < -21.2$ (Blanton & Roweis 2007). The same selection criteria were used in previous papers (Zehavi et al. 2005; Eisenstein et al. 2005; Okumura et al. 2008; Kazin et al. 2010a). The sample we use is referred to as “DR7full” in Kazin et al. (2010a). Our sample includes 87000 LRGs in the redshift range 0.16-0.44.

Spectra cannot be obtained for objects closer than 55 arcsec within a single spectroscopic tile due to the finite size of the fibers. To correct for these “collisions”, the redshift of an object that failed to be measured would be assigned to be the same as the nearest successfully observed one. Both fiber collision corrections and K-corrections have been made in NYU-VAGC (Blanton et al. 2005). The collision corrections applied here are different from what has been suggested in Zehavi et al. (2005). However, the effect should be small since we are using relatively large scale which are less affected by the collision corrections.

We construct the radial selection function as a cubic spline fit to the observed number density histogram with the width $\Delta z = 0.01$. The NYU-VAGC provides the description of the geometry and completeness of the survey in terms of spherical polygons. We adopt it as the angular selection function of our sample. We drop the regions with completeness below 60% to avoid unobserved plates (Zehavi et al. 2005). The Southern Galactic Cap (SGC) region is also dropped because it consists of three non-contiguous stripes in all, and only half as many mocks are available if we include the SGC in our analysis.

3 METHODOLOGY

In this section, we describe the measurement of the multipoles of the correlation function from the observational data, construction of the theoretical prediction, and the likelihood analysis that leads to constraints on dark energy and cosmological parameters.

3.1 Measuring the Two-Dimensional Two-Point Correlation Function

We convert the measured redshifts of galaxies to comoving distances by assuming a fiducial model, Λ CDM with $\Omega_m = 0.25$. We use the two-point correlation function (2PCF) estimator given by Landy & Szalay (1993):

$$\xi(\sigma, \pi) = \frac{DD(\sigma, \pi) - 2DR(\sigma, \pi) + RR(\sigma, \pi)}{RR(\sigma, \pi)}, \quad (1)$$

where π is the separation along the line of sight (LOS), σ is the separation in the plane of the sky, DD, DR, and RR represent the normalized data-data, data-random, and random-random pair counts respectively in a distance range. The LOS is defined as the direction from the observer to the center of a pair. The bin size we use here is $1 h^{-1} \text{Mpc} \times 1 h^{-1} \text{Mpc}$. The Landy and Szalay estimator has minimal variance for a Poisson process. Random data are generated with the same radial and angular selection functions as the real data. One can reduce the shot noise due to random data by increasing the number of random data. The number of random data we use is 10 times that of the real data. While calculating the pair counts, we assign to each data point a radial weight of $1/[1 + n(z) \cdot P_w]$, where $n(z)$ is the radial selection function and $P_w = 4 \cdot 10^4 h^{-3} \text{Mpc}^3$ (Eisenstein et al. 2005). The weight function is included to minimize the variance of clustering measurements for an inhomogeneous sample (Feldman, Kaiser, & Peacock 1994).

3.2 Theoretical Two-Dimensional Two-Point Correlation Function

We compute the linear power spectra by using CAMB (Lewis, Challinor, & Lasenby 2000). To include the effect of non-linear structure formation on the BAOs, we first calculate the dewiggled power spectrum

$$P_{dw}(k) = P_{lin}(k) \exp\left(-\frac{k^2}{2k_*^2}\right) + P_{nw}(k) \left[1 - \exp\left(-\frac{k^2}{2k_*^2}\right)\right], \quad (2)$$

where $P_{lin}(k)$ is the linear matter power spectrum, $P_{nw}(k)$ is the no-wiggle or pure CDM power spectrum calculated using Eq.(29) from Eisenstein & Hu (1998), and k_* is marginalized over with a flat prior over the range of 0.09 to 0.13.

We then use the software package *halofit* (Smith et al. 2003) to compute the non-linear matter power spectrum:

$$r_{halofit}(k) \equiv \frac{P_{halofit,nw}(k)}{P_{nw}(k)} \quad (3)$$

$$P_{nl}(k) = P_{dw}(k)r_{halofit}(k), \quad (4)$$

where $P_{halofit,nw}(k)$ is the power spectrum obtained by applying halofit to the no-wiggle power spectrum, and $P_{nl}(k)$ is the non-linear power spectrum. We compute the theoretical real space two-point correlation function, $\xi(r)$, by Fourier transforming the non-linear power spectrum $P_{nl}(k)$.

In the linear regime (i.e., large scales) and adopting the small-angle approximation (which is valid on scales of interest), the 2D correlation function in the redshift space can be written as (Kaiser 1987; Hamilton 1992)

$$\xi^*(\sigma, \pi) = \xi_0(s)P_0(\mu) + \xi_2(s)P_2(\mu) + \xi_4(s)P_4(\mu), \quad (5)$$

where $s = \sqrt{\sigma^2 + \pi^2}$, μ is the cosine of the angle between $\mathbf{s} = (\sigma, \pi)$ and the LOS, and P_l are Legendre polynomials. The multipoles of ξ could be expressed as

$$\xi_0(r) = \left(1 + \frac{2\beta}{3} + \frac{\beta^2}{5}\right) \xi(r), \quad (6)$$

$$\xi_2(r) = \left(\frac{4\beta}{3} + \frac{4\beta^2}{7}\right) [\xi(r) - \bar{\xi}(r)], \quad (7)$$

$$\xi_4(r) = \frac{8\beta^2}{35} \left[\xi(r) + \frac{5}{2}\bar{\xi}(r) - \frac{7}{2}\bar{\bar{\xi}}(r)\right], \quad (8)$$

where β is the redshift space distortion parameter and

$$\bar{\xi}(r) = \frac{3}{r^3} \int_0^r \xi(r')r'^2 dr', \quad (9)$$

$$\bar{\bar{\xi}}(r) = \frac{5}{r^5} \int_0^r \xi(r')r'^4 dr'. \quad (10)$$

Next, we convolve the 2D correlation function with the distribution function of random pairwise velocities, $f(v)$, to obtain the final model $\xi(\sigma, \pi)$ (Peebles 1980)

$$\xi(\sigma, \pi) = \int_{-\infty}^{\infty} \xi^* \left(\sigma, \pi - \frac{v}{H(z)a(z)} \right) f(v) dv, \quad (11)$$

where the random motions are represented by an exponential form (Ratcliffe et al. 1998; Landy 2002)

$$f(v) = \frac{1}{\sigma_v \sqrt{2}} \exp\left(-\frac{\sqrt{2}|v|}{\sigma_v}\right), \quad (12)$$

where σ_v is the pairwise peculiar velocity dispersion.

The parameter set we use to compute the theoretical correlation function is $\{H(z), D_A(z), \beta, \Omega_m h^2, \Omega_b h^2, n_s, \sigma_v, k_*\}$,

where Ω_m and Ω_b are the density fractions of matter and baryons, n_s is the powerlaw index of the primordial matter power spectrum, and h is the dimensionless Hubble constant ($H_0 = 100h$ km s⁻¹Mpc⁻¹). We set $h = 0.7$ while calculating the non-linear power spectra. On the scales we use for comparison with data, the theoretical correlation function only depends on cosmic curvature and dark energy through parameters $H(z)$, $D_A(z)$, and $\beta(z)$, assuming that dark energy perturbations are unimportant (valid in the simplest dark energy models). Thus we are able to extract constraints from data that are independent of a dark energy model and cosmic curvature.

3.3 Effective Multipoles of the Correlation Function

From Eqs.(5) and (11), we define

$$\begin{aligned} \hat{\xi}_l(s) &\equiv \int_{-\infty}^{\infty} dv f(v) \xi_l \left(\sqrt{\sigma^2 + \left[\pi - \frac{v}{H(z)a(z)} \right]^2} \right) \\ &= \frac{2l+1}{2} \int_{-1}^1 d\mu \xi(\sigma, \pi) P_l(\mu) \\ &= \frac{2l+1}{2} \int_0^\pi d\theta \sqrt{1-\mu^2} \xi(\sigma, \pi) P_l(\mu), \end{aligned} \quad (13)$$

where $\mu = \cos \theta$, and $P_l(\mu)$ is the Legendre Polynomial ($l=0, 2, 4,$ and 6 here). Note that we are integrating over a spherical shell with radius s , while actual measurements of $\xi(\sigma, \pi)$ are done in discrete bins. To compare the measured $\xi(\sigma, \pi)$ and its theoretical model on the same footing, we convert the last integral in Eq.(13) into a sum. This leads to our definition for the effective multipoles of the correlation function:

$$\hat{\xi}_l(s) \equiv \frac{\sum_{s-\frac{\Delta s}{2} < \sqrt{\sigma^2 + \pi^2} < s + \frac{\Delta s}{2}} (2l+1)\xi(\sigma, \pi) P_l(\mu) \sqrt{1-\mu^2}}{\text{Number of bins used in the numerator}}, \quad (14)$$

where $\Delta s = 5 h^{-1}$ Mpc in this work, and

$$\sigma = \left(n + \frac{1}{2}\right) h^{-1} \text{Mpc}, \quad n = 0, 1, 2, \dots \quad (15)$$

$$\pi = \left(m + \frac{1}{2}\right) h^{-1} \text{Mpc}, \quad m = 0, 1, 2, \dots \quad (16)$$

$$\mu \equiv \frac{\pi}{\sqrt{\sigma^2 + \pi^2}}. \quad (17)$$

Note that both the measurements and the theoretical predictions for the effective multipoles are computed using Eq.(14), with $\xi(\sigma, \pi)$ given by the measured correlation function (see Eq.(1)) for the measured effective multipoles, and Eqs.(5)-(11) for their theoretical predictions. We do not use the conventional definitions of multipoles to extract parameter constraints as they use continuous integrals. Bias could be introduced if the definitions of multipoles are different between measurements from data and the theoretical model.

3.4 Covariance Matrix

We use the 160 mock catalogs from the LasDamas simulations² (McBride et al., in preparation) to estimate the covariance matrix

² <http://lss.phy.vanderbilt.edu/lasdamas/>

of the observed correlation function. LasDamas provides mock catalogs matching SDSS main galaxy and LRG samples. We use the LRG mock catalogs from the LasDamas gamma release with the same cuts as the SDSS LRG DR7full sample, $-23.2 < M_g < -21.2$ and $0.16 < z < 0.44$. We have diluted the mock catalogs to match the radial selection function of the observational data by randomly selecting the mock galaxies according to the number density of the data sample. We calculate the multipoles of the correlation functions of the mock catalogs and construct the covariance matrix as

$$C_{ij} = \frac{1}{N-1} \sum_{k=1}^N (\bar{X}_i - X_i^k)(\bar{X}_j - X_j^k), \quad (18)$$

where N is the number of the mock catalogs, \bar{X}_m is the mean of the m^{th} element of the vector from the mock catalog multipoles, and X_m^k is the value in the m^{th} elements of the vector from the k^{th} mock catalog multipoles. The data vector \mathbf{X} is defined by

$$\mathbf{X} = \{\hat{\xi}_0^{(1)}, \hat{\xi}_0^{(2)}, \dots, \hat{\xi}_0^{(N)}; \hat{\xi}_2^{(1)}, \hat{\xi}_2^{(2)}, \dots, \hat{\xi}_2^{(N)}; \dots\}, \quad (19)$$

where N is the number of data points in each measured multipole; $N = 16$ in this work. The length of the data vector \mathbf{X} depends on how many multipoles are used.

3.5 Likelihood

The likelihood is taken to be proportional to $\exp(-\chi^2/2)$ (Press et al. 1992), with χ^2 given by

$$\chi^2 \equiv \sum_{i,j=1}^{N_X} [X_{th,i} - X_{obs,i}] C_{ij}^{-1} [X_{th,j} - X_{obs,j}] \quad (20)$$

where N_X is the length of the vectors X_{th} and X_{obs} , which represent the theoretical model and the observational data respectively.

As explained in Chuang & Wang (2012), instead of recalculating the observed correlation function for different theoretical models, we rescale the theoretical correlation function to avoid rendering χ^2 values arbitrary. The rescaled theoretical correlation function is computed by

$$T^{-1}(\xi_{th}(\sigma, \pi)) = \xi_{th} \left(\frac{D_A(z)}{D_A^{fid}(z)} \sigma, \frac{H^{fid}(z)}{H(z)} \pi \right), \quad (21)$$

where ξ_{th} is given by eq. (11). Hence χ^2 can be rewritten as

$$\chi^2 \equiv \sum_{i,j=1}^{N_X} \{T^{-1}X_{th,i} - X_{obs,i}^{fid}\} C_{fid,ij}^{-1} \cdot \{T^{-1}X_{th,j} - X_{obs,j}^{fid}\}, \quad (22)$$

where $T^{-1}X_{th}$ is a vector given by eq. (21) with ξ_{th} replaced by its effective multipoles (defined by eq. (14)), and X_{obs}^{fid} is the corresponding vector from observational data measured assuming the fiducial model in converting redshifts to distances. See Chuang & Wang (2012) for a more detailed description of our rescaling method.

3.6 Markov Chain Monte Carlo Likelihood Analysis

We use CosmoMC in a Markov Chain Monte Carlo likelihood analysis (Lewis & Bridle 2002). The parameter space that we explore spans the parameter set of $\{H(0.35), D_A(0.35), \Omega_m h^2, \beta, \Omega_b h^2, n_s, \sigma_v, k_*\}$. Only $\{H(0.35), D_A(0.35), \Omega_m h^2, \beta\}$ are

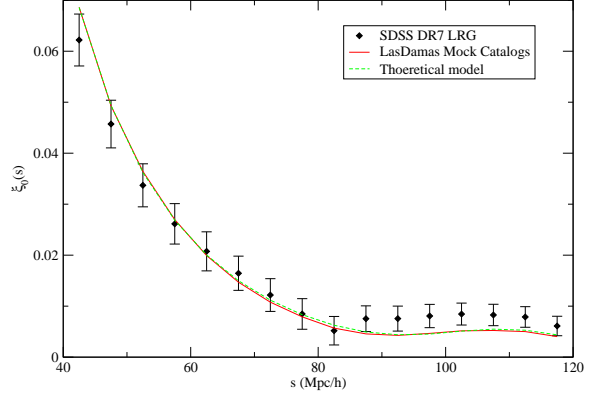


Figure 1. Measurement of monopole of the correlation function of the SDSS DR7 LRG (diamond data points), compared to the average monopole of the correlation functions of the mock catalogs (solid line) and the theoretical model with the input parameters of the simulations (green dashed line). The error bars are taken to be the square roots of the diagonal elements of the covariance matrix.

well constrained using SDSS LRGs alone in the scale range of interest. We marginalize over the other parameters, $\{\Omega_b h^2, n_s, \sigma_v, k_*\}$, with the flat priors, $\{(0.01859, 0.02657), (0.865, 1.059), (0, 500)s^{-1}\text{km}, (0.09, 0.13)h\text{Mpc}^{-1}\}$, where the flat priors of $\Omega_b h^2$ and n_s are centered on the measurements from WMAP7 and has width of $\pm 7\sigma_{WMAP}$ (with σ_{WMAP} from Komatsu et al. (2010)). These priors are wide enough to ensure that CMB constraints are not double counted when our results are combined with CMB data (Chuang, Wang, & Hemantha 2012). We also marginalize over the amplitude of the galaxy correlation function, effectively marginalizing over a linear galaxy bias.

4 RESULTS

4.1 Measurement of multipoles

Figs.1, 2, 3, and 4 show the effective monopole ($\hat{\xi}_0$), quadrupole ($\hat{\xi}_2$), hexadecapole ($\hat{\xi}_4$), and hexacontatetrapole ($\hat{\xi}_6$) measured from SDSS LRGs, compared with the average effective multipoles measured from the mock catalogs. We use the same scale range as Chuang & Wang (2012) ($s = 40 - 120 h^{-1}\text{Mpc}$) for comparison and the bin size used is $5 h^{-1}\text{Mpc}$. The data points from the multipoles in the scale range considered are combined to form a vector, \mathbf{X} (see equation(19)).

We find that $\xi_4(s)$ deviates on scales of $s < 60 \text{ Mpc}/h$ from the measurement from mock data (in contrast to $\xi_0(s)$, $\xi_2(s)$, and $\xi_6(s)$). We note that there are 10 out of 160 mocks which have at least one bin between $40 < s < 55 h^{-1}\text{Mpc}$ for which the amplitude of $\xi_4(s)$ is smaller than -0.01 . Therefore, this deviation could be due to the statistical variance.

A frequently used combination of the monopole and the quadrupole is the normalized quadrupole, defined by

$$Q(s) = \frac{\xi_2(s)}{\xi_0(s) - (3/s^3) \int_0^s \xi_0(s') s'^2 ds'}. \quad (23)$$

For comparison with previous work, we measure the effective normalized quadrupole defined by

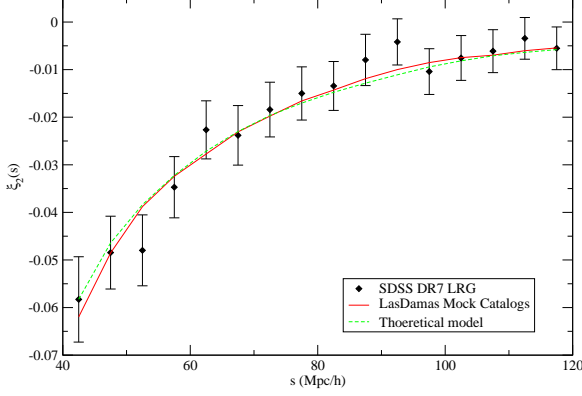


Figure 2. Measurement of quadrupole of the correlation function of the SDSS DR7 LRG (diamond data points), compared to the average quadrupole of the correlation functions of the mock catalogs (red solid line) and the theoretical model with the input parameters of the simulations (green dashed line). The error bars are taken to be the square roots of the diagonal elements of the covariance matrix.

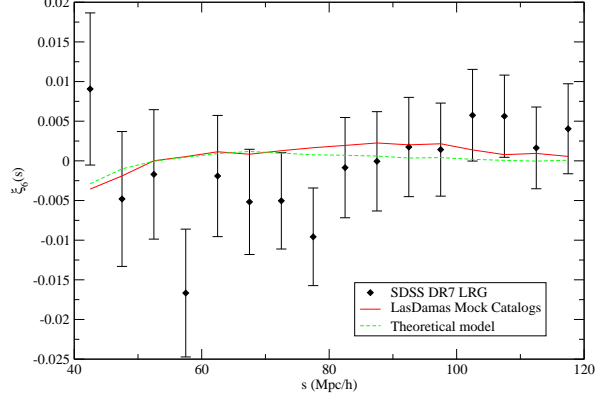


Figure 4. Measurement of hexacontatetrapole of the correlation function of the SDSS DR7 LRG (diamond data points), compared to the average hexacontatetrapole of the correlation functions of the mock catalogs (red solid line) and the theoretical model with the input parameters of the simulations (green dashed line). The error bars are taken to be the square roots of the diagonal elements of the covariance matrix.

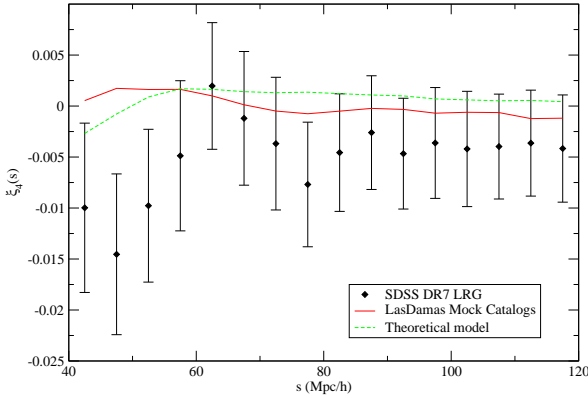


Figure 3. Measurement of hexadecapole of the correlation function of the SDSS DR7 LRG (diamond data points), compared to the average hexadecapole of the correlation functions of the mock catalogs (red solid line) and the theoretical model with the input parameters of the simulations (green dashed line). The error bars are taken to be the square roots of the diagonal elements of the covariance matrix.

$$\hat{Q}(s) \equiv \frac{\hat{\xi}_2(s)}{\hat{\xi}_0(s) - (3/s^3) \sum_{0 < s' \leq s} \hat{\xi}_0(s') s'^2 \Delta s}, \quad (24)$$

from SDSS LRGs (see Fig.5). It is in good agreement with the expectation from the LasDamas mocks, as well as with previous work by Samushia et al. (2011).

4.2 Measurement of $\{H(0.35), D_A(0.35), \beta(0.35)\}$

We now present the model independent measurements of the parameters $\{H(0.35), D_A(0.35), \Omega_m h^2, \beta\}$, obtained by us-

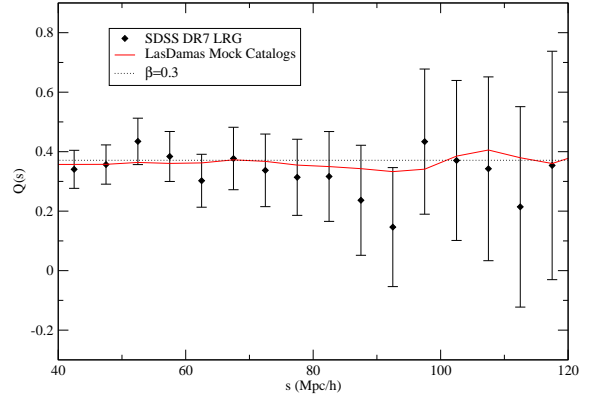


Figure 5. Measurement of the normalized quadrupole from the SDSS DR7 LRG (diamond data points), compared to the mean measurement from the mock catalogs (red solid line). The error bars are taken to be the square roots of the diagonal elements of the covariance matrix. The green dashed line is the theoretical prediction for $\beta = 0.3$ assuming linear power spectrum and small-angle approximation.

ing the method described in previous sections. We also present constraints on the derived parameters $H(0.35) r_s(z_d)/c$ and $D_A(0.35)/r_s(z_d)$, which are more tightly constrained.

4.2.1 Validation Using Mock Catalogs

We first validate our method using mock catalogs. We have applied it to the first 40 LasDamas mock catalogs (which are indexed with

01a-40a)³. Again, we apply the flat and wide priors ($\pm 7\sigma_{WMAP7}$) on $\Omega_b h^2$ and n_s , centered on the input values of the simulation ($\Omega_b h^2 = 0.0196$ and $n_s = 1$).

Table 1 shows the means and standard deviations of the distributions of our measurements of $\{H(0.35), D_A(0.35), \Omega_m h^2, \beta, H(0.35) r_s(z_d)/c, D_A(0.35)/r_s(z_d)\}$ from each monopole + quadrupole ($\hat{\xi}_0 + \hat{\xi}_2$) of the LasDamas mock catalogs of the SDSS LRG sample. The measurements using monopole + quadrupole + hexadecapole ($\hat{\xi}_0 + \hat{\xi}_2 + \hat{\xi}_4$) and monopole + quadrupole + hexadecapole + hexacontatetrapole ($\hat{\xi}_0 + \hat{\xi}_2 + \hat{\xi}_4 + \hat{\xi}_6$) are shown in the same table as well. These are consistent with the input parameters, establishing the validity of our method. In addition, we count the number of the measurements which are outside 1σ from the input values of the simulations. The measurements include $H(0.35)$, $D_A(0.35)$, and $\Omega_m h^2$ from all three methods, $\hat{\xi}_0 + \hat{\xi}_2$, $\hat{\xi}_0 + \hat{\xi}_2 + \hat{\xi}_4$, and $\hat{\xi}_0 + \hat{\xi}_2 + \hat{\xi}_4 + \hat{\xi}_6$. The average percentage is 0.34, close to 0.32, the value we would expect assuming Gaussian distributions. Note that there is a small difference ($\sim 0.5\sigma$) between the restored value and the input value for $D_A(z)/r_s(z_d)$; it should be possible to remove this by using a more accurate model for redshift space distortions, e.g., as described in Reid et al. (2011). However, applying such models is too computationally expensive in our method. We will investigate alternative approaches in future work.

While the constraints from using $\hat{\xi}_0 + \hat{\xi}_2 + \hat{\xi}_4$ are significantly tighter than using $\hat{\xi}_0 + \hat{\xi}_2$, the constraints from using $\hat{\xi}_0 + \hat{\xi}_2 + \hat{\xi}_4 + \hat{\xi}_6$ are nearly the same as that from using $\hat{\xi}_0 + \hat{\xi}_2 + \hat{\xi}_4$. This indicates that $\hat{\xi}_0 + \hat{\xi}_2 + \hat{\xi}_4$ captures nearly all of the information that can be extracted from the data given the noise level. Since linear theory predicts that $\hat{\xi}_l = 0$ for $l > 4$, it is not surprising that $\hat{\xi}_0$, $\hat{\xi}_2$, and $\hat{\xi}_4$ capture most of the information from the 2D 2PCF.

In principle, one could obtain better constraints by including more multipoles. However, the tradeoff is introducing noise to the covariance matrix which could be a problem, since the number of the mock catalogs used to construct the covariance matrix is not big enough. We also show the measurements of $H(0.35) r_s(z_d)/c$, $D_A(0.35)/r_s(z_d)$, $\Omega_m h^2$, and β of each mock catalog in Fig. 6, Fig. 7, Fig. 8, and Fig. 9 to show the scattering among different mock catalogs and the deviations among different methods. One can see that the measurements from different methods are consistent for most mock catalogs, but there are still some obvious deviations ($> 1\sigma$) for a few mock catalogs.

An important point to note is that since the mock data do not include unknown systematic effects, the mean values of estimated parameters remain nearly unchanged as more multipoles measured from data are added to the analysis and the parameter constraints are tightened with the addition of information.

Finally, we compare with the work of Kazin et al. (2012), who measured $H(z)$ and $D_A(z)$ using the average multipoles of the correlation function from the LasDamas mock catalogs. They assume a larger survey volume (~ 12 times) by dividing the covariance matrix by $\sqrt{160}$. They use the average multipoles of the correlation function from the mock catalogs as the theoretical model, which is equivalent to fixing $\Omega_m h^2$, $\Omega_b h^2$, and n_s to the input parameters of the simulations. We fix the damping factor, $k_* = 0.13 h\text{Mpc}^{-1}$, and the pairwise peculiar velocity dispersion, $\sigma_v = 300 \text{ s}^{-1}\text{km}$, which give a good fit to the average correlation function of the mock catalogs. Corresponding to the bottom panel of fig. 6

³ We only use 40 instead of 160 mock catalogs because the MCMC is computationally expensive. However, the covariance matrix is constructed with 160 mock catalogs.

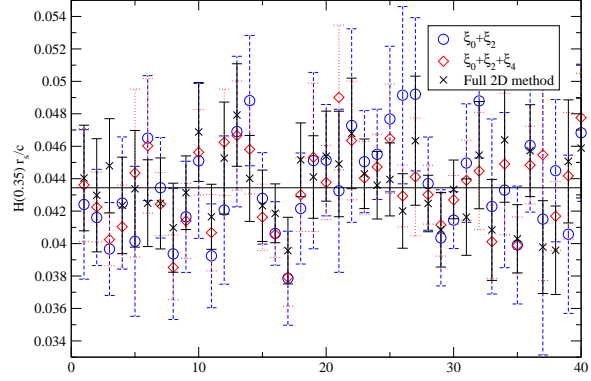


Figure 6. Measurements of the means and standard deviation of $H(0.35) r_s(z_d)/c$ from 40 individual mock catalogs (indexed as 01a to 40a). The blue circles show the measurements using $\hat{\xi}_0 + \hat{\xi}_2$. The red diamonds show the measurements using $\hat{\xi}_0 + \hat{\xi}_2 + \hat{\xi}_4$. The black crosses show the measurements using full 2D 2PCF method from our previous work. The black line shows the theoretical value computed with the input parameters of the simulations.

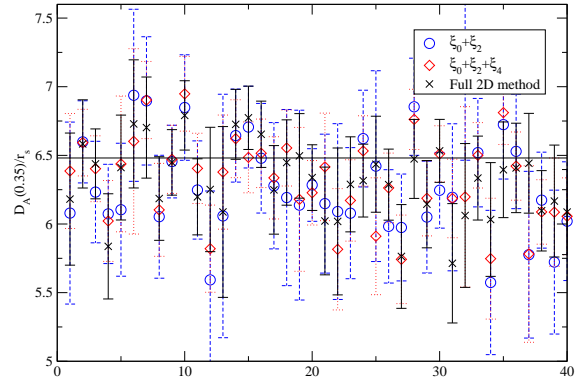


Figure 7. Measurements of the means and standard deviation of $D_A(0.35) r_s(z_d)$ from 40 individual mock catalogs (indexed as 01a to 40a). The blue circles show the measurements using $\hat{\xi}_0 + \hat{\xi}_2$. The red diamonds show the measurements using $\hat{\xi}_0 + \hat{\xi}_2 + \hat{\xi}_4$. The black crosses show the measurements using full 2D 2PCF method from our previous work. The black line shows the theoretical value computed with the input parameters of the simulations.

in Kazin et al. (2012), we measure the hubble parameter and angular diameter distance by marginalizing over the amplitude of the correlation function and the linear redshift space distortion parameter and using the scale range, $s = 40 - 150 h^{-1}\text{Mpc}$. Our results are shown in Fig. 10, and are similar to theirs. The 1-D marginalized uncertainties of $\{H, D_A, \beta\}$ we measure using $\hat{\xi}_0 + \hat{\xi}_2 + \hat{\xi}_4$ is $\{1.17\%, 0.81\%, 4.45\%\}$ which are similar to their results, $\{1.42\%, 0.76\%, 4.95\%\}$ (the numbers are taken from Fig. 7 in Kazin et al. (2012)). They derive the theoretical multipoles analytically, instead of using the same definition applied to the observational data. In principle, it could introduce biases to the mea-

	$\hat{\xi}_0 + \hat{\xi}_2$	$\hat{\xi}_0 + \hat{\xi}_2 + \hat{\xi}_4$	$\hat{\xi}_0 + \hat{\xi}_2 + \hat{\xi}_4 + \hat{\xi}_6$	input value
$H(0.35)$	81.1 ± 5.6	80.4 ± 4.9	80.3 ± 5.1	81.79
$D_A(0.35)$	1017 ± 63	1027 ± 56	1021 ± 48	1032.8
$\Omega_m h^2$	0.119 ± 0.014	0.116 ± 0.013	0.116 ± 0.013	0.1225
β	0.325 ± 0.076	0.327 ± 0.066	0.324 ± 0.075	–
$H(0.35) r_s(z_d)/c$	0.0436 ± 0.0030	0.0435 ± 0.0025	0.0434 ± 0.0026	0.0434
$D_A(0.35)/r_s(z_d)$	6.29 ± 0.36	6.31 ± 0.31	6.28 ± 0.26	6.48

Table 1. The mean and standard deviation of the distribution of the measured values of $\{H(0.35), D_A(0.35), \Omega_m h^2, \beta, H(0.35) r_s(z_d)/c, D_A(0.35)/r_s(z_d)\}$ from each $\hat{\xi}_0 + \hat{\xi}_2$, $\hat{\xi}_0 + \hat{\xi}_2 + \hat{\xi}_4$, or $\hat{\xi}_0 + \hat{\xi}_2 + \hat{\xi}_4 + \hat{\xi}_6$ of 40 LasDamas mock catalogs (which are indexed with 01a-40a). Our measurements are consistent with the input values within 1σ , where each σ is computed from the 40 means measured from the 40 mock catalogs. The unit of H is $\text{km s}^{-1} \text{Mpc}^{-1}$. The unit of D_A and $r_s(z_d)$ is Mpc.

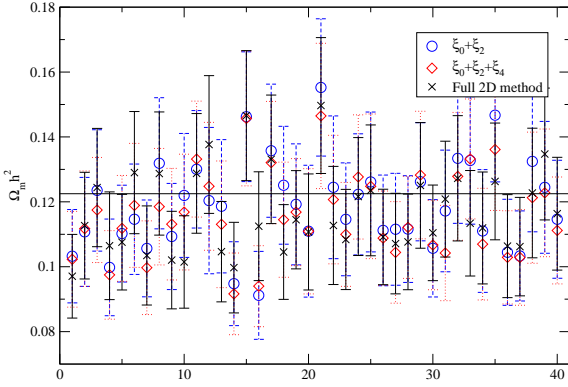


Figure 8. Measurements of the means of $\Omega_m h^2$ from 40 individual mock catalogs (indexed as 01a to 40a). The blue circles show the measurements using $\hat{\xi}_0 + \hat{\xi}_2$. The red diamonds show the measurements using $\hat{\xi}_0 + \hat{\xi}_2 + \hat{\xi}_4$. The black crosses show the measurements using full 2D 2PCF method from our previous work. The black line shows the theoretical value computed with the input parameters of the simulations.

measurements. However, the effect might be minimized since they construct the theoretical model based on the measured multipoles from the mock catalogs, which is equivalent to computing the theoretical multipoles with the same definition applied to the observational data.

4.2.2 Measurements from SDSS DR7 LRG

Table 2 lists the mean, rms variance, and 68% confidence level limits of the parameters, $\{H(0.35), D_A(0.35), \Omega_m h^2, \beta, H(0.35) r_s(z_d)/c, D_A(0.35)/r_s(z_d)\}$, derived in an MCMC likelihood analysis from the measured $\hat{\xi}_0 + \hat{\xi}_2$ of the correlation function of the SDSS LRG sample. Table 3 lists the mean, rms variance, and 68% confidence level limits of the same parameter set from the measured $\hat{\xi}_0 + \hat{\xi}_2 + \hat{\xi}_4$ of the correlation function of the SDSS LRG sample for this parameter set. The χ^2 per degree of freedom ($\chi^2/\text{d.o.f.}$) is 1.23 for $\hat{\xi}_0 + \hat{\xi}_2$ and is 1.06 for $\hat{\xi}_0 + \hat{\xi}_2 + \hat{\xi}_4$. These are independent of a dark energy model, and obtained without assuming a flat Universe. There are obvious deviations between the cosmological constraints obtained from the measured $\hat{\xi}_0 + \hat{\xi}_2$ and $\hat{\xi}_0 + \hat{\xi}_2 + \hat{\xi}_4$ of the correlation function of the

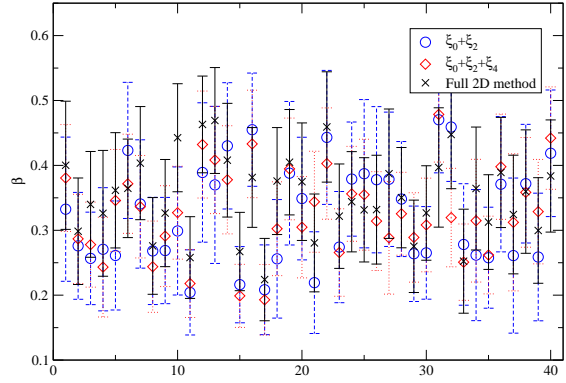


Figure 9. Measurements of the means of β from 40 individual mock catalogs (indexed as 01a to 40a). The blue circles show the measurements using $\hat{\xi}_0 + \hat{\xi}_2$. The red diamonds show the measurements using $\hat{\xi}_0 + \hat{\xi}_2 + \hat{\xi}_4$. The black crosses show the measurements using full 2D 2PCF method from our previous work.

SDSS LRG sample, i.e. $\{\Delta\beta = 0.10, \Delta H(0.35) r_s(z_d)/c = 0.0037, \Delta D_A(0.35)/r_s(z_d) = 0.31\}$. To explore how significant these deviations are, we compute the standard deviations of these differences from Fig. 6, 7, and 9 and find $\{\sigma(\Delta\beta) = 0.049, \sigma(\Delta H(0.35) r_s(z_d)/c) = 0.0024, \sigma(\Delta D_A(0.35)/r_s(z_d)) = 0.24\}$. One can see that the differences from the measurements are around 1 to 2 σ . Thus the deviations between Table 2 and Table 3 could be due to statistical variance.

Table 4 gives the normalized covariance matrix for this parameter set measured using $\hat{\xi}_0 + \hat{\xi}_2$. While the measurement of β , 0.44 ± 0.15 , seems to be higher than what we expect (i.e. $\beta = 0.325 \pm 0.076$ from the mock catalogs using $\hat{\xi}_0 + \hat{\xi}_2$), note that there is a negative correlation between β and $\Omega_m h^2$ and the correlation coefficient is -0.2549 . Thus the somewhat high β value is mildly correlated with the somewhat low $\Omega_m h^2$ value. In addition, the somewhat high β value is actually still statistically consistent with the measurement from the mock catalogs. The most robust measurements are that of $\{H(0.35) r_s(z_d)/c, D_A(0.35)/r_s(z_d)\}$, same as in Chuang & Wang (2012). These can be used to combine with other data sets and constraining dark energy and cosmological parameters, see Wang, Chuang & Mukherjee (2012).

Fig. 11 shows one and two-dimensional marginalized con-

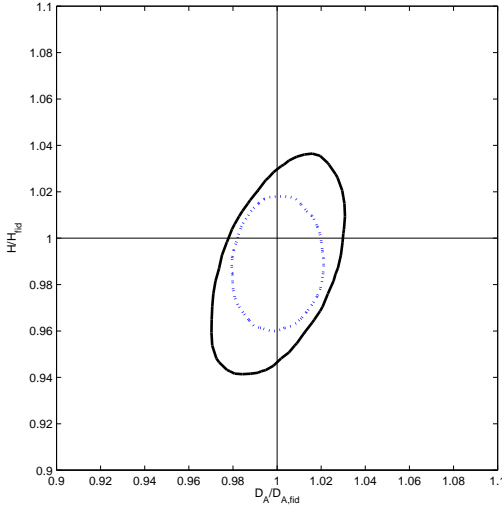


Figure 10. 2D marginalized contours (95% C.L.) for $D_A(z)/D_A^{true}$ and $H(z)/H^{true}$ for the comparison with fig. 6 in Kazin et al. (2012). The black solid contour is measured using $\hat{\xi}_0 + \hat{\xi}_2$ and the blue dotted contour is measured using $\hat{\xi}_0 + \hat{\xi}_2 + \hat{\xi}_4$. Our constraints are similar with the results in Kazin et al. (2012).

	mean	σ	lower	upper
$H(0.35)$	79.6	8.8	70.9	87.8
$D_A(0.35)$	1060	92	970	1150
$\Omega_m h^2$	0.103	0.015	0.088	0.118
β	0.44	0.15	0.29	0.59
$H(0.35) r_s(z_d)/c$	0.0435	0.0045	0.0391	0.0477
$D_A(0.35)/r_s(z_d)$	6.44	0.51	5.99	6.90

Table 2. The mean, standard deviation, and the 68% C.L. bounds of $\{H(0.35), D_A(0.35), \Omega_m h^2, \beta, H(0.35) r_s(z_d)/c, D_A(0.35)/r_s(z_d)\}$ from SDSS DR7 LRGs using $\hat{\xi}_0 + \hat{\xi}_2$. The unit of H is $\text{km s}^{-1} \text{Mpc}^{-1}$. The unit of D_A and $r_s(z_d)$ is Mpc.

tours of the parameters, $\{H(0.35), D_A(0.35), \Omega_m h^2, \beta, H(0.35) r_s(z_d)/c, D_A(0.35)/r_s(z_d)\}$, derived in an MCMC likelihood analysis from the measured $\hat{\xi}_0 + \hat{\xi}_2$ of the SDSS LRG sample.

	mean	σ	lower	upper
$H(0.35)$	87.3	6.7	80.8	93.7
$D_A(0.35)$	1095	59	1037	1153
$\Omega_m h^2$	0.107	0.015	0.093	0.122
β	0.54	0.11	0.44	0.65
$H(0.35) r_s(z_d)/c$	0.0472	0.0033	0.0441	0.0503
$D_A(0.35)/r_s(z_d)$	6.75	0.25	6.52	6.98

Table 3. The mean, standard deviation, and the 68% C.L. bounds of $\{H(0.35), D_A(0.35), \Omega_m h^2, \beta, H(0.35) r_s(z_d)/c, D_A(0.35)/r_s(z_d)\}$ from SDSS DR7 LRGs using $\hat{\xi}_0 + \hat{\xi}_2 + \hat{\xi}_4$. The unit of H is $\text{km s}^{-1} \text{Mpc}^{-1}$. The unit of D_A and $r_s(z_d)$ is Mpc.

4.3 Comparison with Previous Work

While we have developed a general method to measure the dark energy and cosmological parameters that could be extracted from the galaxy clustering data alone, we restrict our method now by fixing some parameters to obtain the results for comparison with previous work.

In our previous paper (Chuang & Wang 2012), we used full 2D correlation function and measured $H(z = 0.35) = 82.1_{-4.9}^{+4.8} \text{ km s}^{-1} \text{Mpc}^{-1}$ and $D_A(z = 0.35) = 1048_{-58}^{+60} \text{ Mpc}$, which are consistent with this study; note that the full 2D correlation function captures more information than the leading multipoles. Xu et al. (2012) applied the density field reconstruction method on the same data and obtained $H(z = 0.35) = 84.4 \pm 7.1$ and $D_A(z = 0.35) = 1050 \pm 38 \text{ Mpc}$, which are also in excellent agreement with our measurements.

Cabre & Gaztanaga (2009) measure β from SDSS DR6 LRG using the normalized quadrupole defined by Eq.(23). To compare with their results, we make similar assumptions, and use monopole-quadrupole method with fixing $\Omega_m = 0.25$, $\Omega_b = 0.045$, $h = 0.72$, $n_s = 0.98$, $k_* = 0.11$, and $\sigma_v = 300 \text{ km/s}$ in the Λ CDM model ($H(0.35)$ and $D_A(0.35)$ would also be fixed accordingly). Considering the scale range, $s = 40 - 100 h^{-1} \text{ Mpc}$, we obtain $\beta = 0.333 \pm 0.055$, in excellent agreement with their measurement of $\beta = 0.34 \pm 0.05$. Since the definition of the normalized quadrupole includes an integral of monopole with the minimum boundary from $s = 0$, the advantage of using our effective multipole method instead of normalized quadrupole method is to avoid the distortion from the small scales where the scale dependent uncertainties are not well known. However, the distortion might be negligible compared to the statistical uncertainty of current measurements.

Song et al. (2011) split the same galaxy sample (SDSS DR7 LRG) to two redshift slices and obtained $\beta(z = 0.25) = 0.30_{-0.048}^{+0.047}$ and $\beta(z = 0.38) = 0.39 \pm 0.056$ without considering the geometric distortions. Their results are in excellent agreement with the values measured by Cabre & Gaztanaga (2009) and us under the same assumptions. In addition, Blake et al. (2011) measured $H(z) D_A(z)(1+z)/c = 0.28 \pm 0.04$ and 0.44 ± 0.07 at $z = 0.22$ and 0.41 respectively from WiggleZ survey (Blake et al. 2009; Parkinson et al. 2012). Linearly interpolating their results, we find the mean of $H(z) D_A(z)(1+z)/c$ to be 0.39 at $z=0.35$, which is in excellent agreement with our measurement of $H(0.35) D_A(0.35)(1.35)/c = 0.38 \pm 0.06$.

5 SYSTEMATICS

Table. 5 shows the systematic tests that we have carried out by varying key assumptions made in our analysis. These include the multipoles used, the range of scales used, the bin size used, and the minimum of the transverse separation used to calculate the correlation function.

We use the results using $\hat{\xi}_0 + \hat{\xi}_2$ as our fiducial results. We find that the constraints are stronger for using $\hat{\xi}_0 + \hat{\xi}_2 + \hat{\xi}_4$, but using $\hat{\xi}_0 + \hat{\xi}_2 + \hat{\xi}_6$ does not improve the constraints significantly. Therefore, it seems that $\hat{\xi}_0 + \hat{\xi}_2 + \hat{\xi}_4$ contains most of the information from the 2D 2PCF. Since the measurements of $\hat{\xi}_0 + \hat{\xi}_2 + \hat{\xi}_4$ deviate from those of $\hat{\xi}_0 + \hat{\xi}_2$ by about 1σ , we use the latter as our fiducial results to be conservative.

We vary the scale range chosen and the bin size used and find that the results are basically consistent. However, we find

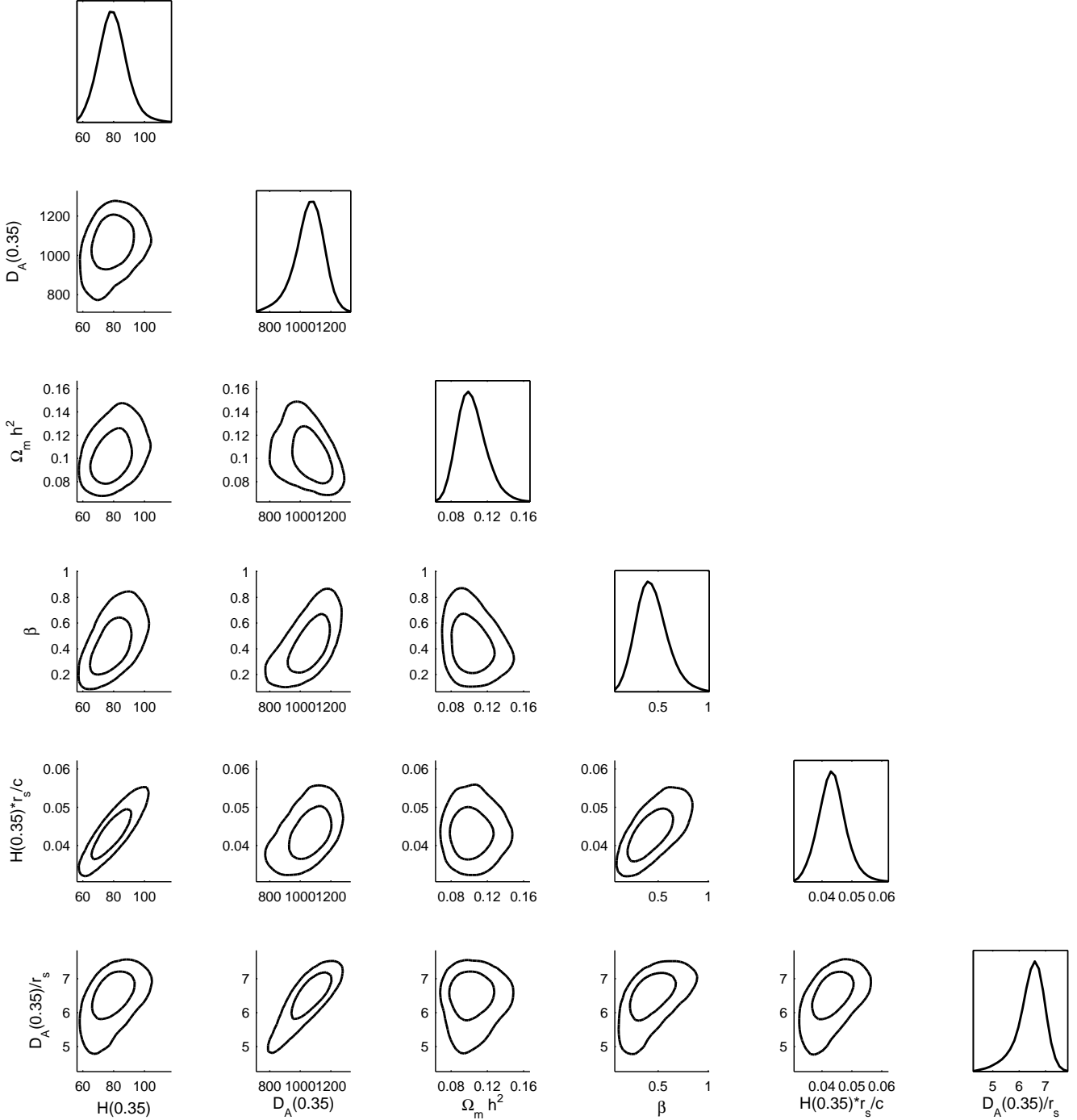


Figure 11. 2D marginalized contours (68% and 95% C.L.) for $\{H(0.35), D_A(0.35), \Omega_m h^2, \beta, H(0.35) r_s(z_d)/c, D_A(0.35)/r_s(z_d)\}$. The diagonal panels represent the marginalized probabilities. The unit of H is $\text{km s}^{-1} \text{Mpc}^{-1}$. The unit of D_A and $r_s(z_d)$ is Mpc.

that the measurement of $D_A(z)/r_s(z_d)$ is more stable than that of $H(0.35) r_s(z_d)/c$. It might indicate the appearance of systematic errors from the measurement of the correlation function in the direction along the line of sight. While the observed correlation function along the line of sight is noisier and harder to model due to galaxy peculiar velocities, we test the impact of systematic uncertainties along the line of sight by removing the data with the transverse separation, σ , smaller than 5 or $10 h^{-1} \text{Mpc}$. We find that the results are insensitive to this. Thus our measurement of

$H(0.35) r_s(z_d)/c$ should not be contaminated by systematic errors along the line of sight.

There is possible systematic uncertainty from the radial selection function used to construct the random catalogs. Ross et al. (2012) found that the least biased way is using "shuffled" method for SDSS-III/BOSS DR9 CMASS sample. Shuffled method is to assign the redshift of a galaxy of the random catalog with the redshift of the observed data picked randomly. Samushia et al. (2012) found that using spline method, which is the same method as we

	$H(0.35)$	$D_A(0.35)$	$\Omega_m h^2$	β	$H(0.35) r_s(z_d)/c$	$D_A(0.35)/r_s(z_d)$
$H(0.35)$	1	0.2669	0.3529	0.5802	0.9259	0.4832
$D_A(0.35)$	0.2669	1	-0.3835	0.6307	0.4586	0.8814
$\Omega_m h^2$	0.3529	-0.3835	1	-0.2549	-0.0057	0.07
β	0.5802	0.6307	-0.2549	1	0.7176	0.575
$H(0.35) r_s(z_d)/c$	0.9259	0.4586	-0.0057	0.7176	1	0.4981
$D_A(0.35)/r_s(z_d)$	0.4832	0.8814	0.07	0.575	0.4981	1

Table 4. Normalized covariance matrix of the measured and derived parameters, $\{H(0.35), D_A(0.35), \Omega_m h^2, \beta, H(0.35) r_s(z_d)/c, D_A(0.35)/r_s(z_d)\}$ from SDSS DR7 LRGs using $\xi_0 + \xi_2$.

use in this study, could obtain less biased result for SDSS DR7 LRG sample. In fact, the biased effect due to the radial selection function depends on the galaxy sample, survey geometry, and scale range studied. For example, for a narrow beam survey, while most of the structure is in the line of sight direction, shuffled method would erase most of the information. Samushia et al. (2012) showed that the spline method has least bias for the SDSS DR7 LRG sample in the scale range we are interested ($s > 40h^{-1}\text{Mpc}$). And the bias is much smaller than the statistic error. Therefore, we expect the bias to be negligible.

6 CONCLUSION AND DISCUSSION

We have demonstrated the feasibility of using multipoles of the correlation function to measure $H(z)$, $D_A(z)$, $\Omega_m h^2$, and β by applying the method to individual mock catalogs from LasDamas in an MCMC likelihood analysis.

The method we developed is modified from Chuang & Wang (2012), which was the first method to include the geometric distortion (also known as Alcock-Paczynski test, see Alcock & Paczynski (1979)) on galaxy clustering data on large scales. We compute the multipoles from the theoretical and observed 2D 2PCF in the same way, thus the only approximation made is that the distance of any pair of galaxies can be converted with two stretch factors between different models in the redshift range considered.

We have obtained the constraints for the measured and derived parameters, $\{H(0.35), D_A(0.35), \Omega_m h^2, \beta, H(0.35) r_s(z_d)/c, D_A(0.35)/r_s(z_d)\}$, from the multipoles of the correlation function from the sample of SDSS DR7 LRGs which are summarized by Tables 2 and 3.

We find that while the mean values of estimated parameters remain stable (with rare deviations) for the mock data when higher multipoles are used, this is not true for the SDSS DR7 LRG data. We find $H(0.35) r_s(z_d)/c = 0.0437_{-0.0043}^{+0.0041}$ using monopole + quadrupole, and $H(0.35) r_s(z_d)/c = 0.0472 \pm 0.0031$ using monopole + quadrupole + hexadecapole. This deviation could be caused by statistical variance. In addition, there is some deviation between the LasDamas measurements and the theoretical model for hexadecapole. However, the deviation is small compared to the uncertainties of the measurements. To be conservative, we choose the measurement using monopole + quadrupole as our fiducial results.

ACKNOWLEDGEMENTS

We are grateful to the LasDamas project for making their mock catalogs publicly available. The computing for this project was per-

formed at the OU Supercomputing Center for Education and Research (OSCAR) at the University of Oklahoma (OU). This work used the Extreme Science and Engineering Discovery Environment (XSEDE), which is supported by National Science Foundation grant number OCI-1053575. This work was supported by DOE grant DE-FG02-04ER41305. C.C. was also supported by the Spanish MICINN's Consolider-Ingenio 2010 Programme under grant MultiDark CSD2009-00064 and grant AYA2010-21231, and by the Comunidad de Madrid under grant HEPHACOS S2009/ESP-1473.

Funding for the Sloan Digital Sky Survey (SDSS) has been provided by the Alfred P. Sloan Foundation, the Participating Institutions, the National Aeronautics and Space Administration, the National Science Foundation, the U.S. Department of Energy, the Japanese Monbukagakusho, and the Max Planck Society. The SDSS Web site is <http://www.sdss.org/>.

The SDSS is managed by the Astrophysical Research Consortium (ARC) for the Participating Institutions. The Participating Institutions are The University of Chicago, Fermilab, the Institute for Advanced Study, the Japan Participation Group, The Johns Hopkins University, Los Alamos National Laboratory, the Max-Planck-Institute for Astronomy (MPIA), the Max-Planck-Institute for Astrophysics (MPA), New Mexico State University, University of Pittsburgh, Princeton University, the United States Naval Observatory, and the University of Washington.

REFERENCES

- Abazajian, K. N., *et al.* [SDSS Collaboration], *Astrophys. J. Suppl.* **182**, 543 (2009) [arXiv:0812.0649 [astro-ph]].
- Alcock, C., and Paczynski, B., *Nature* **281**, 358 (1979).
- Anderson, L.; Aubourg, E.; Bailey, S.; Bizyaev, D.; Blanton, M.; Bolton, A. S.; Brinkmann, J.; and Brownstein, J. R. *et al.*, *Mon. Not. Roy. Astron. Soc.* **428**, 1036 (2013) [arXiv:1203.6594 [astro-ph.CO]].
- Bacon DJ, Refregier AR, Ellis RS *MNRAS* 318:625 (2000)
- Bennett, C. L., *et al.*, *Astrophys. J. Suppl.* **148**, 1 (2003)
- Blake, C., Glazebrook, K, 2003, *ApJ*, 594, 665
- Blake, C.; Collister, A.; Bridle, S.; and Lahav, O., *Mon. Not. Roy. Astron. Soc.* **374**, 1527 (2007) [arXiv:astro-ph/0605303].
- Blake, C., *et al.* 2009, *MNRAS*, 395, 240
- C. Blake, K. Glazebrook, T. Davis, S. Brough, M. Colless, C. Contreras, W. Couch and S. Croom *et al.*, *Mon. Not. Roy. Astron. Soc.* **418**, 1725 (2011) [arXiv:1108.2637 [astro-ph.CO]].
- Blanton, M. R., *et al.* [SDSS Collaboration], *Astron. J.* **129**, 2562 (2005) [arXiv:astro-ph/0410166].
- Blanton, M. R.; and Roweis, S., *Astron. J.* **133**, 734 (2007) [arXiv:astro-ph/0606170].

	$H(0.35)$	$D_A(0.35)$	$\Omega_m h^2$	β	$H(0.35) r_s(z_d)/c$	$D_A(0.35)/r_s(z_d)$
$\hat{\xi}_0 + \hat{\xi}_2$ (fiducial)	$80.0^{+8.2}_{-8.6}$	1063^{+87}_{-85}	0.103 ± 0.015	$0.45^{+0.15}_{-0.14}$	$0.0437^{+0.0041}_{-0.0043}$	$6.48^{+0.44}_{-0.43}$
$\hat{\xi}_0 + \hat{\xi}_2 + \hat{\xi}_4$	87.3 ± 6.4	1095 ± 58	$0.107^{+0.015}_{-0.014}$	0.54 ± 0.11	0.0472 ± 0.0031	$6.75^{+0.24}_{-0.23}$
$\hat{\xi}_0 + \hat{\xi}_2 + \hat{\xi}_6$	$78.5^{+8.7}_{-8.9}$	1025^{+88}_{-82}	0.107 ± 0.016	0.41 ± 0.14	$0.0424^{+0.0044}_{-0.0043}$	6.31 ± 0.49
$30 < s < 120$	$85.1^{+7.8}_{-8.2}$	1072^{+64}_{-62}	0.115 ± 0.014	0.38 ± 0.10	$0.0453^{+0.0037}_{-0.0039}$	$6.71^{+0.31}_{-0.30}$
$50 < s < 120$	$77.5^{+8.2}_{-8.4}$	1034^{+103}_{-109}	$0.101^{+0.019}_{-0.018}$	$0.5^{+0.19}_{-0.18}$	$0.0425^{+0.0038}_{-0.0040}$	$6.27^{+0.55}_{-0.61}$
$40 < s < 110$	$73.5^{+6.7}_{-7.0}$	1064^{+77}_{-76}	0.107 ± 0.015	0.35 ± 0.11	$0.0398^{+0.0031}_{-0.0034}$	$6.54^{+0.41}_{-0.40}$
$40 < s < 130$	$83.5^{+8.3}_{-8.7}$	1082^{+78}_{-75}	0.105 ± 0.015	0.48 ± 0.15	$0.0454^{+0.0041}_{-0.0043}$	$6.63^{+0.37}_{-0.35}$
bin size = $4 h^{-1}$ Mpc	$77.3^{+7.1}_{-7.2}$	1026^{+86}_{-85}	0.113 ± 0.017	0.39 ± 0.12	0.0413 ± 0.0034	6.39 ± 0.45
bin size = $8 h^{-1}$ Mpc	$79.1^{+8.1}_{-8.6}$	1065^{+84}_{-78}	0.112 ± 0.017	0.42 ± 0.13	$0.0423^{+0.0039}_{-0.0041}$	$6.62^{+0.41}_{-0.37}$
$\sigma > 5 h^{-1}$ Mpc	$79.6^{+8.3}_{-8.4}$	1054^{+87}_{-85}	0.103 ± 0.015	0.43 ± 0.14	0.0434 ± 0.0042	$6.43^{+0.45}_{-0.42}$
$\sigma > 10 h^{-1}$ Mpc	$76.5^{+7.5}_{-7.8}$	1048 ± 84	0.099 ± 0.014	0.37 ± 0.13	$0.0420^{+0.0036}_{-0.0039}$	6.34 ± 0.44
$\frac{\text{mean}_{\text{max}} - \text{mean}_{\text{min}}}{(\sigma_{\text{fid}}^+ + \sigma_{\text{fid}}^-)/2}$	1.64	0.81	1.07	1.31	1.76	1.01

Table 5. This table shows the systematic tests that vary the combination of multipoles, the scale range, the bin size, and the minimum transverse separation used in the analysis. The fiducial results are obtained using $\hat{\xi}_0 + \hat{\xi}_2$, the scale range $40 < s < 120 h^{-1}$ Mpc, a bin size of $5 h^{-1}$ Mpc, and no minimum transverse separation. The other results are calculated with only specified quantities different from the fiducial one. The unit of H is $\text{km s}^{-1} \text{Mpc}^{-1}$. The unit of D_A and $r_s(z_d)$ is Mpc. In the last row, we show the variation between these tests by computing the maximum difference between the mean values divided by the errors of the fiducial measurements.

- Cabre, A.; and Gaztanaga, E., *Mon. Not. Roy. Astron. Soc.* **393**, 1183 (2009) [arXiv:0807.2460 [astro-ph]].
- Chuang, C.-H.; Wang, Y.; and Hemantha, M. D. P., *MNRAS*, **423**, 1474 (2012)
- Chuang, C.-H. and Wang, Y. *MNRAS*, **426**, 226 (2012)
- Cimatti, A.; Robberto, M.; Baugh, C. M.; Beckwith, S. V. W.; Content, R.; Daddi, E.; De Lucia, G.; and Garilli B. *et al.*, *Exper. Astron.* **23**, 39 (2009) [arXiv:0804.4433 [astro-ph]].
- Colless, M., *et al.* [The 2DFGRS Collaboration], *Mon. Not. Roy. Astron. Soc.* **328**, 1039 (2001) [arXiv:astro-ph/0106498].
- Colless, M.; Peterson, B. A.; Jackson, C.; Peacock, J. A.; Cole, S.; Norberg, P.; Baldry, I. K.; and Baugh, C. M. *et al.*, *astro-ph/0306581*.
- Eisenstein, D. J.; and Hu, W., *Astrophys. J.* **496**, 605 (1998) [arXiv:astro-ph/9709112].
- Eisenstein, D. J., *et al.* [SDSS Collaboration], *Astron. J.* **122**, 2267 (2001) [arXiv:astro-ph/0108153].
- Eisenstein, D. J., *et al.* [SDSS Collaboration], *Astrophys. J.* **633**, 560 (2005) [arXiv:astro-ph/0501171].
- Eisenstein, D.J., *et al.*, 2011, arXiv:1101.1529v1 [astro-ph.IM]
- H. A. Feldman, N. Kaiser and J. A. Peacock, *Astrophys. J.* **426**, 23 (1994) [astro-ph/9304022].
- Fukugita, M.; Ichikawa, T.; Gunn, J. E.; Doi, M.; Shimasaku, K.; and Schneider, D. P., *Astron. J.* **111**, 1748 (1996).
- Gaztanaga, E.; Cabre, A.; and Hui, L. *Mon. Not. Roy. Astron. Soc.* **399**, 1663 (2009) [arXiv:0807.3551 [astro-ph]].
- Gunn, J. E., *et al.* [SDSS Collaboration], *Astron. J.* **116**, 3040 (1998) [arXiv:astro-ph/9809085].
- Gunn, J. E., *et al.* [SDSS Collaboration], *Astron. J.* **131**, 2332 (2006) [arXiv:astro-ph/0602326].
- Hamilton, A. J. S., 1992, *APJL*, **385**, L5
- Hutsi, G., arXiv:astro-ph/0507678.
- Kaiser, N., *Mon. Not. Roy. Astron. Soc.* **227**, 1 (1987).
- Kaiser N, Wilson G, Luppino GA arXiv:astro-ph/0003338 (2000)
- Kazin, E. A., *et al.*, *Astrophys. J.* **710**, 1444 (2010) [arXiv:0908.2598 [astro-ph.CO]].
- Kazin, E. A.; Blanton, M. R.; Scoccimarro, R.; McBride, C. K.; and Berlind, A. A., *Astrophys. J.* **719**, 1032 (2010) [arXiv:1004.2244 [astro-ph.CO]].
- Kazin, E. A.; Sanchez, A. G.; and Blanton, M. R. *Mon. Not. Roy. Astron. Soc.* **419**, 3223 (2012) [arXiv:1105.2037 [astro-ph.CO]].
- Roy. Astron. Soc. **419**, 3223 (2012) [arXiv:1105.2037 [astro-ph.CO]].
- Komatsu, E. *et al.* [WMAP Collaboration], *Astrophys. J. Suppl.* **192**, 18 (2011) [arXiv:1001.4538 [astro-ph.CO]].
- Landy, S. D. and Szalay, A. S., *Astrophys. J.* **412**, 64 (1993).
- Landy, S. D., “The Pairwise Velocity Distribution Function of Galaxies in the LCRS, 2dF, *Astrophys. J.* **567**, L1 (2002) [arXiv:astro-ph/0202130].
- Laureijs, R., *et al.*, “Euclid Definition Study Report”, arXiv:1110.3193
- Lewis, A.; Challinor, A.; and Lasenby, A., *Astrophys. J.* **538**, 473 (2000) [arXiv:astro-ph/9911177].
- Lewis, A. and Bridle, S., *Phys. Rev. D* **66**, 103511 (2002) [arXiv:astro-ph/0205436].
- Manera, M.; Scoccimarro, R.; Percival, W. J.; Samushia, L.; McBride, C. K.; Ross, A.; Sheth, R.; and White, M. *et al.*, *Mon. Not. Roy. Astron. Soc.* **428**, 2, 1036 (2012). [arXiv:1203.6609 [astro-ph.CO]].
- Martinez, V. J., *et al.*, *Astrophys. J.* **696**, L93 (2009) [Erratum-ibid. **703**, L184 (2009)] [Astrophys. J. **703**, L184 (2009)] [arXiv:0812.2154 [astro-ph]].
- Montesano, F.; Sanchez, A. G.; and Phleps, S., *Mon. Not. Roy. Astron. Soc.* **421**, 2656 (2012) [arXiv:1107.4097 [astro-ph.CO]].
- S. E. Nuza, A. G. Sanchez, F. Prada, A. Klypin, D. J. Schlegel, S. Gottloeber, A. D. Montero-Dorta and M. Manera *et al.*, arXiv:1202.6057 [astro-ph.CO].
- Okumura, T.; Matsubara, T.; Eisenstein, D. J.; Kayo, I.; Hikage, C.; Szalay, A. S.; and Schneider, D. P., *Astrophys. J.* **676**, 889 (2008) [arXiv:0711.3640 [astro-ph]].
- Padmanabhan, N., *et al.* [SDSS Collaboration], *Mon. Not. Roy. Astron. Soc.* **378**, 852 (2007) [arXiv:astro-ph/0605302].
- Padmanabhan, N.; Xu, X.; Eisenstein, D. J.; Scalzo, R.; Cuesta, A. J.; Mehta, K. T.; and Kazin, E., *Mon. Not. Roy. Astron. Soc.* **427**, 3, 2132 (2012) [arXiv:1202.0090 [astro-ph.CO]].
- D. Parkinson, S. Riemer-Sorensen, C. Blake, G. B. Poole, T. M. Davis, S. Brough, M. Colless and C. Contreras *et al.*, *Phys. Rev. D* **86**, 103518 (2012) [arXiv:1210.2130 [astro-ph.CO]].
- Peebles, P. J. E. 1980, *The Large-Scale Structure of the Universe* (Princeton, NJ: Princeton University Press)

- Percival, W. J.; Cole, S.; Eisenstein, D. J.; Nichol, R. C.; Peacock, J. A.; Pope, A. C.; and Szalay, A. S., *Mon. Not. Roy. Astron. Soc.* **381**, 1053 (2007) [arXiv:0705.3323 [astro-ph]].
- Percival, W. J., *et al.*, *Mon. Not. Roy. Astron. Soc.* **401**, 2148 (2010) [arXiv:0907.1660 [astro-ph.CO]].
- Perlmutter, S., *et al.* [Supernova Cosmology Project Collaboration], *Astrophys. J.* **517**, 565 (1999) [arXiv:astro-ph/9812133].
- Press W.H., Teukolsky S.A., Vetterling W.T., Flannery B.P., 1992, *Numerical recipes in C. The art of scientific computing*, Second edition, Cambridge: University Press.
- Ratcliffe, A., *et al.*, 1998, *VizieR Online Data Catalog*, 730, 417
- Reid, B. A.; Percival, W. J.; Eisenstein, D. J.; Verde, L.; Spergel, D. N.; Skibba, R. A.; Bahcall, N. A.; and Budavari, T. *et al.*, *Mon. Not. Roy. Astron. Soc.* **404**, 60 (2010) [arXiv:0907.1659 [astro-ph.CO]].
- B. A. Reid and M. White, *Mon. Not. Roy. Astron. Soc.* **417**, 1913 (2011) [arXiv:1105.4165 [astro-ph.CO]].
- B. A. Reid, L. Samushia, M. White, W. J. Percival, M. Manera, N. Padmanabhan, A. J. Ross and A. G. Sanchez *et al.*, arXiv:1203.6641 [astro-ph.CO].
- Riess, A. G., *et al.* [Supernova Search Team Collaboration], *Astron. J.* **116**, 1009 (1998) [arXiv:astro-ph/9805201].
- Ross, A. J. *et al.* [BOSS Collaboration], *Mon. Not. Roy. Astron. Soc.* **424**, 564 (2012) [arXiv:1203.6499 [astro-ph.CO]].
- Sanchez, A. G.; Crocce, M.; Cabre, A.; Baugh, C. M.; and Gaztanaga, E., *Mon. Not. Roy. Astron. Soc.* **400**, 1634 (2009) [arXiv:0901.2570 [astro-ph]].
- Sanchez, A. G.; Scoccola, C. G.; Ross, A. J.; Percival, W.; Manera, M.; Montesano, F.; Mazzalay, X.; and Cuesta, A. J. *et al.*, *Mon. Not. Roy. Astron. Soc.* **425**, 415 (2012) [arXiv:1203.6616 [astro-ph.CO]].
- Samushia, L.; Percival, W. J.; and Raccanelli, A., *Mon. Not. Roy. Astron. Soc.* **420**, 2102 (2012) [arXiv:1102.1014 [astro-ph.CO]].
- Samushia, L.; Reid, B. A.; White, M.; Percival, W. J.; Cuesta, A. J.; Lombriser, L.; Manera, M.; and Nichol, R. C. *et al.*, *Mon. Not. Roy. Astron. Soc.* **429**, 1514 (2013) [arXiv:1206.5309 [astro-ph.CO]].
- Saunders, W., *et al.*, *Mon. Not. Roy. Astron. Soc.* **317**, 55 (2000) [arXiv:astro-ph/0001117].
- Seo, H. and Eisenstein, D. J., 2003, *ApJ*, 598, 720
- Smith, R. E., *et al.* [The Virgo Consortium Collaboration], *Mon. Not. Roy. Astron. Soc.* **341**, 1311 (2003) [arXiv:astro-ph/0207664].
- Song, Y. -S.; Sabiu, C. G.; Kayo, I.; and Nichol, R. C., *JCAP* **1105**, 020 (2011) [arXiv:1006.4630 [astro-ph.CO]].
- Tegmark, M., *et al.* [SDSS Collaboration], *Astrophys. J.* **606**, 702 (2004) [arXiv:astro-ph/0310725].
- R. Tojeiro, W. J. Percival, J. Brinkmann, J. R. Brownstein, D. Eisenstein, M. Manera, C. Maraston and C. K. McBride *et al.*, *Mon. Not. Roy. Astron. Soc.* **424**, 2339 (2012) arXiv:1203.6565 [astro-ph.CO].
- Van Waerbeke, L., *et al.* *Astron. Astrophys* 358:30 (2000)
- Wang, Y., 2006, *ApJ*, 647, 1
- Wang, Y., *et al.*, *MNRAS*, 409, 737 (2010)
- Wang, Y.; Chuang, C. -H.; and Mukherjee, P., *Phys. Rev. D* **85**, 023517 (2012) [arXiv:1109.3172 [astro-ph.CO]].
- Wittman, D. M.; Tyson, J. A.; Kirkmand, D.; Dell'Antonio, I.; Bernstein, G., *Nature*, 405, 143 (2000)
- X. Xu, A. J. Cuesta, N. Padmanabhan, D. J. Eisenstein and C. K. McBride, arXiv:1206.6732 [astro-ph.CO].
- Zehavi, I., *et al.* [SDSS Collaboration], *Astrophys. J.* **621**, 22 (2005) [arXiv:astro-ph/0411557].